A Comparison of Human Body Wearable Sensor Positions for UWB-based Indoor Localization

Timothy Otim[1], Luis E. Díez[1], Alfonso Bahillo[1], Peio Lopez-Iturri[2], and Francisco Falcone[2]

[1] Faculty of Engineering, University of Deusto, Avda. Universidades 24, 48007, Bilbao, Spain
{otim.timothy, luis.enrique.diez, alfonso.bahillo}@deusto.es
[2] Department of Electric, Electronic and Communication Engineering, Public University of Navarra, Campus de Arrosadia, 31006, Pamplona, Spain
{peio.lopez, francisco.falcone}@unavarra.es

Abstract. Over the years, several UWB localization systems have already been proposed for accurate position estimation of pedestrians. Most of these systems already proposed for pedestrian localization have only been individually evaluated for a particular wearable sensor position. In this paper, we compare the positioning performance of seven body wearable sensor positions i.e., chest, arm, ankle, wrist, thigh, fore-head, and hand using an Extended Kalman Filter (EKF) based localization algorithm in an indoor environment. The conclusion drawn is that the fore-head is the best, and the chest is the worst body sensor location for tracking a pedestrian. While the fore-head position is able to set an error lower than 0.35 m (90^{th} percentile), the chest is able to set 4 m. The fore-head's performance is followed by the hand, ankle, wrist, thigh, arm, and chest in that order.

Keywords: UWB · Localization · Body Wearable Sensors · Human body shadowing.

1 Introduction

Wearable connected devices hold a great deal of promise, and therefore their market is expected to reach $ 70 billion in 2025 [1]. The major sectors in this market are consumer electronics, defences, and healthcare. Some of the popular wearable sensors that are widely used include: gyroscope and accelerometer sensors for navigation purposes and proximity sensors to detect if a defined subject or obstacle is present nearby. Therefore, one of the key application of wearables is in tracking of pedestrians [2].

Indoor localization of pedestrians is still an open problem though many different approaches have been proposed using diverse technologies to obtain a similar performance to the Global Navigation Satelite System (GNSS) outdoors. For instance, Wi-Fi, Ultrawideband (UWB), or Ultrasound, and advanced processing techniques, such as Kalman and Particle Filters, have been proposed to cope with the deterioration in performance due to combined effects of pathloss and multipath fading. Among the most accurate localization solutions are those that rely on ultrasound or UWB radio signals but both their performances deteriorate in non-line-of sight (NLOS). UWB signals can achieve decimeter-level errors in indoor positioning and has gained significant interest in research as a promising candidate for industry solutions. In recent years, there has been a great deal of interest in its use for positioning [3–5].

However, in tracking context of pedestrians using UWB technology, an important factor which has been often overlooked but has significant effect on the positioning error is the influence caused by the human body itself. The effects of human body shadowing are additional propagation losses or biases in time of flight (TOF) measurements when the body blocks the line-of-sight (LOS) between a wearable sensor and an anchor. These effects, which generally depend on: i) body

wearable sensor position, and ii) relative heading angle are currently, not adequately accounted for and will decrease the accuracy of localization systems.

In recent years, a few works have focused on the ranging and positioning error introduced by the human body due to the relative heading angle, leaving aside the impact of body wearable sensor positions [6–10]. Therefore, knowledge of a body wearable sensor position that will provide good accuracy results is important. In this paper, we present a novel comparison of UWB positioning error results for seven body wearable sensor locations namely, fore-head, hand, chest, wrist, arm, thigh and ankle using an Extended Kalman Filter (EKF)-based localization algorithm. The aforementioned body wearable positions are chosen because they are the most popular in the market according to Vandrico database [11].

The rest of this paper is organized as follows: experimental setup and the method adopted to collect the experimental data is described in Section II. The UWB positioning performance is analyzed in sections III for different body wearable sensor positions. In section IV, the presentation and discussion of results is made. Finally, in the last section, we give some conclusions and future work.

2 Experimental Setup

Throughout this paper, several TREK1000 development kits manufactured by Decawave were used. According to [12], TREK1000 development kits are the best UWB commercial products for ranging. The nodes are fully compliant with the IEEE 802.15.4-2011 UWB standard and make it possible to achieve ranging measurements using two-way ranging measurements at a rate of 3.57 Hz. For the purpose of these measurement campaigns, 1 TREK1000 node was configured as a wearable sensor and 4 nodes were configured as anchors and installed at fixed positions in the Lab. The nodes were made to work with a 110 kb/s data rate and in the channel 2 (3990 MHz).

The experiments were carried out inside the Luis Mercader Lab at the department of Electric, Electronic and Communication engineering at the Public University of Navarra in Spain. The Lab had the following dimensions: 6 m wide, 13 m long, and 4 m high, and contained a number of computers, monitors, chairs, desks, closets and working people. The floor and ceiling were made of concrete. The floor plan of lab environment where the tests were performed is showed in Fig. 1.

The floor plan shows detailed anchor positions and a path with 26 ground-truth points with each point approximately 1 m from the other. There are several interfering objects such as pieces of furniture, metallic cabinets and desktop computers. The origin of the reference system is defined at the top left corner. The UWB anchors were mounted on tripods in the positions indicated in Table 1.

Table 1: Coordinates of UWB Anchors, where n is the anchor identity number defined as $n = 0$, 1, 2, 3

Anchor (n)	**X (cm)**	**Y (cm)**	**Z (cm)**
Anchor 0	1240	571	170
Anchor 1	1240	70	173
Anchor 2	548	33	172
Anchor 3	68	21	172

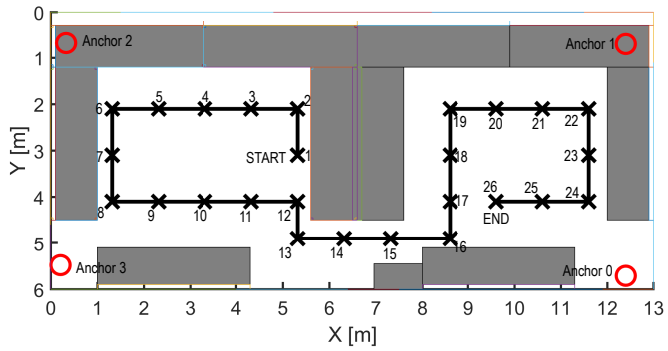

Fig. 1: Map of the room and the installation in Luis Mercader Lab. A path with 26 ground-truth points (marked with crosses) was selected. Also shown are the 4 anchors at the corners of the Lab.

A male subject, 1.80 m height and 77 kg mass was considered for the measurements. The wearable sensors were mounted on the subject with the help of Velcro straps at the right-ankle, right-thigh, fore-head, right-hand, right-arm, chest, and right- wrist as seen in Fig. 2.The heights at which the wearable sensors were mounted are showed in Table 2.

Table 2: Height (H) in centimetres at which the wearable sensors are mounted

	Ankle	Thigh	Fore-head	Hand	Arm	Chest	Wrist
H	15	70	177	120	130	130	90

Using the installed ground marks, firstly, the wearable sensor was mounted on a tripod and moved along the path starting from test point 1 and ending at test point 26 [see – Fig. 1] as a reference for further comparisons.

Similar to the work in [13], for each wearable sensor position, the subject was made to walk the same path, and ranges were recorded continuously without stopping as the subject moved from the start to end. At each ground-truth point, the subject stood still for approximately 10 s before moving to the next.

3 Positioning Performance

Because the main application of ranging is positioning, in this section we compare the positioning performance. As explained in the previous section, the infrastructure of the experiments consists of one UWB node mounted on seven body locations and four UWB nodes in fixed and known positions acting as anchors. In order to achieve the positioning performance, a localization algorithm based on the EKF is implemented. We use range measurements from the continuous scenario. To minimise the effects of NLOS, the measured ranges with a very large error were assumed to be under NLOS conditions. And so, they were rejected in the update of the state vector estimation.

(a) Chest (b) Arm (c) Ankle (d) Wrist (e) Thigh (f) Fore-head (g) Hand

Fig. 2: Wearable sensors mounted at different positions on the body. At the hand, the sensor is about 20 cm from the chest since this is a usual place for texting or looking at the screen of a smart phone when locating your position in a real world scenario.

Similar to [14] and [15], the EKF will consist of a discrete time white noise acceleration driven model as the dynamic model and the ranges between the wearable sensor at different body locations and the anchors as the measurements. The dynamic model is modeled as a constant position model driven by acceleration noise instead of a constant velocity model. The position model driven by acceleration noise is equivalent to having a constant velocity = 0. We chose this model because the subject was still most of the time.

The state vector $\boldsymbol{x}_k$ is defined by the 3-D position ($\boldsymbol{p}$) and velocity ($\boldsymbol{v}$) estimates as indicated in (1) as :

$$\boldsymbol{x}_{k|k} = \boldsymbol{x}_k = (\boldsymbol{p}_k \ \boldsymbol{v}_k \ )^T \tag{1}$$

Therefore, $\boldsymbol{x}_k$ is defined as :

$$\boldsymbol{x}_{k|k-1} = \boldsymbol{F}_k \boldsymbol{x}_{k-1|k-1} + \boldsymbol{w}_k \tag{2}$$

where $\boldsymbol{F}_k$ is the state transition matrix given as :

$$\boldsymbol{F}_k = \begin{pmatrix} 1 & 0 & 0 \\ 0 & 1 & 0 \\ 0 & 0 & 1 \end{pmatrix} \tag{3}$$

$\boldsymbol{w}_k$ is the process noise, modeled as a white noise acceleration with covariance matrix $\boldsymbol{Q}_k$:

$$\boldsymbol{Q}_k = \begin{pmatrix} \sigma_{ax}^2 \Delta T^2/2 & 0 & 0 \\ 0 & \sigma_{ay}^2 \Delta T^2/2 & 0 \\ 0 & 0 & \sigma_{az}^2 \Delta T^2/2 \end{pmatrix} \tag{4}$$

where ΔT is equal to the time difference between timestamps $\boldsymbol{k}$ and $\boldsymbol{k}-1$ and $\sigma_{ax} = 100$ cm, $\sigma_{ay} = 100$ cm , and $\sigma_{az} = 10$ cm are the uncertainty that model the acceleration driving noise of the dynamic model in the x, y, and z directions. The state vector $\boldsymbol{x}_k$ is initialized with the coordinates of the first ground marks. Their initial standard deviations were set to 20 cm for the x and y coordinates, and 0.5 cm for the z coordinate. These parameters were set from preliminary measurements to characterize the UWB nodes and the motion of the subject.

The measurement model has the form:

$$\boldsymbol{z}_k = \boldsymbol{h}(\boldsymbol{x}_{k|k}) + \boldsymbol{n}_k \tag{5}$$

where $\boldsymbol{z}_k$ is the measurements vector, $\boldsymbol{h}$ is the measurement non-linear function, and $\boldsymbol{n}_k$ is the measurement noise with covariance matrix $\boldsymbol{R}_k$.

The standard deviation (SD) of the measurement model was set according to Table 3. The values were obtained from a set of measurements to characterize the UWB nodes for each wearable sensor position.

Using UWB ranges from the 4 anchors to update the estimate of the state $\boldsymbol{x}_{k|k}$, the measurements take on the following form:

$$z_{n,k} = h_n(\boldsymbol{x}_{k|k}) =$$
$$= \sqrt{(p_x - a_{x,n})^2 + (p_y - a_{y,n})^2 + (p_z - a_{z,n})^2} \tag{6}$$

where $z_{n,k}$ is the measured range between the nth anchor at the position $a_{x,n}, a_{y,n}$, $a_{z,n}$, and wearable sensor with current position estimates at p_x, p_y and p_z.

Table 3: The uncertainty in centimetres of the measurement model for each wearable sensor position

	Ankle	Thigh	Fore-head	Hand	Arm	Chest	Wrist
SD	50	60	10	30	50	130	20

Because the output of the EKF filter provides a continuous estimation of the position, it is necessary to detect when the subject feet are still so that the ground truth positions are estimated. Therefore, we performed the following tasks for each of the body wearable positions.

1. Smoothing: where a moving average filter is applied to each position component. The length of the window was empirically set to 4 s.
2. Filtering: in order to reduce the number of outliers in the position estimation, a moving variance with window length of 4 s was also set.
3. To determine the ground truth position, the *k-means* clustering is applied to the filtered estimates. The ground truth positions are extorted from the obtained centroids.

4 Results and Discussion

To compare the performance of the different wearable sensor positions, the absolute value of the difference between the real ground truth positions and the values estimated by the EKF are used as the error metric. To better see the performance results, the main statistics are presented in the Table 4. In Table 4, we differentiate the performance results according to the sensors that worn on the the frontal plane (fore-head, chest and hand) and the side plane (ankle, wrist, thigh, and arm) of the user.

Looking at Table 4, the first observation is the existence of a clear relationship between the localization performance and the body wearable sensor position. Overall, it can be observed that the fore-head and the chest position give the best and worst possible localization performance, respectively. In absolute terms, 90 % of the estimates were below the error of 0.35 m and 4.04 m for the fore-head and chest, respectively.

The performance of the chest is heavily influenced by NLOS conditions due to human body shadowing. Though all the wearable positions are influenced by human body shadowing effect, this effect is more pronounced at the chest because the large size of the chest allows a lot more power to get absorbed by the body, which explicitly translates in to extremely large errors. Therefore, the chest position can be used if it is possible to install enough anchors to minimize the risk of NLOS.

Table 4: Body wearable positions with their estimation errors (in meters). P90 is the 90^{th} percentile.

Body Plane	Body Location	Mean	Median	P90	SD
Front	Fore-head	0.20	0.21	0.35	0.11
	Hand	0.35	0.26	0.62	0.33
	Chest	2.46	2.55	4.04	1.66
Side	Ankle	0.50	0.36	0.97	0.36
	Wrist	0.62	0.52	1.14	0.48
	Thigh	0.68	0.57	1.46	0.45
	Arm	1.36	1.26	2.47	0.77

After the fore-head, the hand position obtains the second lowest errors as 90 % of the estimates were below the error of 0.62 m. The hand performs better than the chest (though in both cases the wearable is at the center of the chest) because the space of 20 cm [see – Fig. 2g] allows for creeping wave propagation during NLOS. Among the wearable positions where the sensor is placed on side plane of the user, the ankle gives the best performance as 90 % of the estimates were below the error of 0.97 m. Following the performance of the ankle position is the wrist, thigh, and arm locations with 90^{th} percentile of 1.14 m, 1.46 m, 2.47 m, respectively. Similar to the ranging performance, the differences in the position errors among these locations can be attributed to the differences in the height and size of the limb on which the sensor is attached.

5 Conclusion

We have presented an experimental comparison of seven body wearable sensor positions available for tracking the position of a pedestrian. The comparison has been done in an indoor environment with LOS and NLOS conditions. Several NLOS have been created by the body of the user which acts as an obstacle of the direct signal path between the wearable sensor and the access point. While the performance of forehead has been superior, the performance results for the chest position has been observed to be lower than the other wearable sensor positions.

References

1. P. Harrop, J. Hayward, R. Das, and G. Holland, *Wearable Technology 2015-2025: Technologies, Markets, Forecast.* IDTechEx Research 2015.
2. S. C. Mukhopadhyay, "Wearable Sensors for Human Activity Monitoring: A Review," *IEEE Sensors Journal*, vol. 15, no. 3, pp. 1321–1330, Mar. 2015.
3. F. Lazzari, A. Buffi, P. Nepa, and S. Lazzari, "Numerical Investigation of an UWB Localization Technique for Unmanned Aerial Vehicles in Outdoor Scenarios," *IEEE Sensors Journal*, vol. 17, no. 9, pp. 2896–2903, May 2017.
4. J. Tiemann, F. Schweikowski, and C. Wietfeld, "Design of an UWB indoor-positioning system for UAV navigation in GNSS-denied environments," in *2015 International Conference on Indoor Positioning and Indoor Navigation (IPIN).* Banff, AB, Canada: IEEE, Oct. 2015, pp. 1–7.
5. H. Perakis and V. Gikas, "Evaluation of Range Error Calibration Models for Indoor UWB Positioning Applications," in *2018 International Conference on Indoor Positioning and Indoor Navigation (IPIN).* Nantes: IEEE, Sep. 2018, pp. 206–212.

6. Y. Kilic, A. J. Ali, A. Meijerink, M. J. Bentum, and W. G. Scanlon, "The effect of human-body shadowing on indoor UWB TOA-based ranging systems." IEEE, Mar. 2012, pp. 126–130.
7. Y. Gengt, "Modeling the effect of human body on TOA ranging for indoor human tracking with wrist mounted sensor," *16th International Symposium on Wireless Personal Multimedia Communications (WPMC), Atlantic City, NJ,*, pp. 1–6, 2013.
8. J. He, Y. Geng, and K. Pahlavan, "Modeling indoor TOA ranging error for body mounted sensors," in *2012 IEEE 23rd International Symposium on Personal, Indoor and Mobile Radio Communications - (PIMRC)*. Sydney, Australia: IEEE, Sep. 2012, pp. 682–686.
9. Q. Tian, K. I.-K. Wang, and Z. Salcic, "Human Body Shadowing Effect on UWB-Based Ranging System for Pedestrian Tracking," *IEEE Transactions on Instrumentation and Measurement*, pp. 1–10, 2018.
10. T. Otim, A. Bahillo, L. E. Díez, P. Lopez-Iturri, and F. Falcone, "FDTD and Empirical Exploration of Human Body and UWB Radiation Interaction on TOF Ranging," *Antennas and Wireless Propagation Letters*, vol. 6, no. 1, p. 5, 2019.
11. "Vandrico Inc. Wearable Technology Database," http://vandrico.com/wearables/wearable-technology-database, accessed: 2019-02-12.
12. A. R. Jimenez Ruiz and F. Seco Granja, "Comparing Ubisense, BeSpoon, and DecaWave UWB Location Systems: Indoor Performance Analysis," *IEEE Transactions on Instrumentation and Measurement*, vol. 66, no. 8, pp. 2106–2117, Aug. 2017.
13. A. R. Jiménez and F. Seco, "Comparing Decawave and Bespoon UWB location systems: indoor/outdoor performance analysis," in *Indoor Positioning and Indoor Navigation (IPIN), 2016 International Conference on*. IEEE, 2016, pp. 1–8.
14. L. E. Diez, A. Bahillo, T. Otim, and J. Otegui, "Step Length Estimation Using UWB Technology: A Preliminary Evaluation," in *2018 International Conference on Indoor Positioning and Indoor Navigation (IPIN)*. Nantes: IEEE, Sep. 2018, pp. 1–8.
15. M. Ridolfi, S. Vandermeeren, J. Defraye, H. Steendam, J. Gerlo, D. De Clercq, J. Hoebeke, and E. De Poorter, "Experimental Evaluation of UWB Indoor Positioning for Sport Postures," *Sensors*, vol. 18, no. 2, p. 168, Jan. 2018.